



## Molecular Crystals and Liquid Crystals

Publication details, including instructions for authors and subscription information:

<http://www.tandfonline.com/loi/gmcl20>

## Antiferroelectric Liquid Crystal with $^{13}\text{C}$ Isotope Studied Using FT-IR Spectroscopy and the Density Functional Theory Calculations

A. Fukuda <sup>a</sup>, J. K. Vij <sup>a</sup>, R. Korlacki <sup>a b</sup>, A. Kocot <sup>a b</sup>,  
B. Jin <sup>c</sup> & Y. Takanishi <sup>c</sup>

<sup>a</sup> Department of Electronic and Electrical Engineering, Trinity College, University of Dublin, Dublin, Ireland

<sup>b</sup> Institute of Physics, University of Silesia, Uniwersytecka, Katowice, Poland

<sup>c</sup> Department of Organic and Polymeric Materials, Tokyo Institute of Technology, Tokyo, Japan

Version of record first published: 31 Aug 2006

To cite this article: A. Fukuda, J. K. Vij, R. Korlacki, A. Kocot, B. Jin & Y. Takanishi (2005): Antiferroelectric Liquid Crystal with  $^{13}\text{C}$  Isotope Studied Using FT-IR Spectroscopy and the Density Functional Theory Calculations, *Molecular Crystals and Liquid Crystals*, 437:1, 269/[1513]-278/[1522]

To link to this article: <http://dx.doi.org/10.1080/15421400590956072>

Full terms and conditions of use: <http://www.tandfonline.com/page/terms-and-conditions>

This article may be used for research, teaching, and private study purposes. Any substantial or systematic reproduction, redistribution, reselling, loan, sub-licensing, systematic supply, or distribution in any form to anyone is expressly forbidden.

The publisher does not give any warranty express or implied or make any representation that the contents will be complete or accurate or up to date. The accuracy of any instructions, formulae, and drug doses should be independently verified with primary sources. The publisher shall not be liable for any loss, actions, claims, proceedings, demand, or costs or damages whatsoever or howsoever caused arising directly or indirectly in connection with or arising out of the use of this material.

## Antiferroelectric Liquid Crystal with $^{13}\text{C}$ Isotope Studied Using FT-IR Spectroscopy and the Density Functional Theory Calculations

**A. Fukuda**

**J. K. Vij**

Department of Electronic and Electrical Engineering, Trinity College, University of Dublin, Dublin, Ireland

**R. Korlacki**

**A. Kocot**

Department of Electronic and Electrical Engineering, Trinity College, University of Dublin, Dublin, Ireland and Institute of Physics, University of Silesia, Uniwersytecka, Katowice, Poland

**B. Jin**

**Y. Takanishi**

Department of Organic and Polymeric Materials, Tokyo Institute of Technology, Tokyo, Japan

*A comparison of infrared spectra obtained experimentally and reproduced using the density functional theory (DFT) calculations for an antiferroelectric liquid crystal 4-(1-methylheptyloxycarbonyl) phenyl 4'-octylcarbonyloxybiphenyl-4-carboxylate (MHPOCBC) is being presented. The material has been prepared for investigations using infrared spectroscopy by exchanging a single carbon atom with the  $^{13}\text{C}$  isotope in order to examine the carbonyl vibrational modes separately. Polarised infrared studies of the homogenously aligned cell show that the peak assigned to the stretching vibration of the carbonyl group in the non-chiral terminal chain exhibits high dichroic ratio. This effect may be explained if the transition dipole moment of this carbonyl band is considered to be exactly perpendicular to the long molecular axis. This has been obtained from the simulated molecular geometry. Such a geometry may play an important role in stabilising the anticlinic order.*

**Keywords:** antiferroelectric liquid crystal; density functional theory; infrared spectroscopy

Address correspondence to J. K. Vij, Department of Electronic and Electrical Engineering, Trinity College, University of Dublin, Dublin 2, Ireland. E-mail: jvij@tcd.ie

## 1. INTRODUCTION

It is possible to reproduce a vibrational spectrum of the molecule using *ab initio* or density functional theory (DFT) calculations. For liquid crystalline molecules, with number of atoms exceeding 50, it is a difficult problem even for current computers. However, analysis of the rich vibrational spectra of such molecules may be much easier, supported by results of molecular modelling calculations. In the present paper we show a comparison of infrared spectra obtained experimentally and reproduced theoretically for an antiferroelectric liquid crystal.

Infrared spectroscopy is a powerful technique for investigating the orientational order of liquid crystals. Kim *et al.* [1] first employed this technique for proving the hindered rotation of carbonyl dipoles about the long molecular axis in several antiferroelectric liquid crystals, and since that date a number of papers have appeared in which the liquid crystalline phases have been discussed. A recent review of these works is given by Kocot *et al.* [2]. In order to understand the origin of antiferroelectricity, most attention is focused on the microscopic structure near the chiral center of molecules. However, according to the model proposed by Osipov *et al.* [3,4], the transversal dipoles localised far from the centre of the molecule and also in the non-chiral tail, play crucial role in stabilising the anticlinic order. A presence of an additional large transversal dipole in the non-chiral tail, which is supported by a conformation obtained from the DFT calculations, may thus promote anticlinic order rather than synclinic one.

## 2. MATERIAL

Material under study was a classic antiferroelectric liquid crystal R-MHPOCBC [5] with carbon atoms in the “core” carbonyl group selectable exchanged with  $^{13}\text{C}$  isotope (Fig. 1). The molecule contains

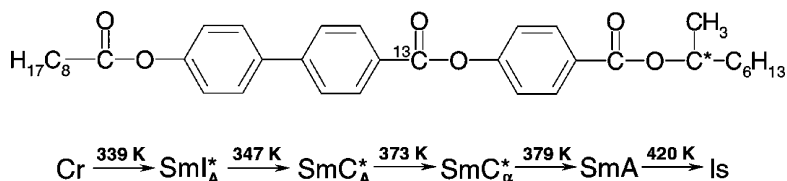


**FIGURE 1** Structure and phase sequence of the MHPOCBC.

three carbonyl groups: in a neighbourhood of the chiral center ("chiral"), inside the molecular core ("core") and in the non-chiral terminal chain ("chain"). It is expected, that selective substitution by the heavier isotope, will shift the vibrational peak to the lower frequencies. It allows us to observe independently three peaks in the range of  $1800\text{--}1680\text{ cm}^{-1}$  one for each of the carbonyl groups.

The sample MHPOCBC is known for its strong antiferroelectric properties [6]. With essentially the same molecular structure as MHPOBC [7] (the only difference being the presence of an additional carbonyl group in the non-chiral tail) the sample does not exhibit any ferroelectric or ferrielectric phases, but three different antiferroelectric ones ( $\text{SmI}_A^*$ ,  $\text{SmC}_A^*$  and  $\text{SmC}_\alpha^*$  phase [8]) are exhibited.

### 3. EXPERIMENT

Infrared experiments were carried out for the homogenously aligned cell. The cell was prepared using ZnSe windows equipped with the indium-tin-oxide (ITO) electrodes. The nylon 6/6 was used as an orienting layer and the mylar film of the thickness of  $5\text{ }\mu\text{m}$  used as spacers. Spectra were collected with the Bio-Rad FTS-6000 Fourier transform infrared spectrometer (FT-IR) using the DTGS detector. The experiments were performed in the  $\text{SmC}_A^*$  phase without applied electric field and in field-induced synclinic phase [9]. A reference spectrum was also collected in the isotropic phase.

### 4. CALCULATIONS

Calculations were carried out using the density functional theory (the Gaussian 98 W application [10]) with the hybrid B3LYP functional [11] and the standard polarised 6-31 G\* basis set. The geometry of single molecule was optimised to obtain the stable conformation and then the vibrational spectrum was calculated. In order to avoid computational approximations, the calculated force field was scaled with the scaled quantum-mechanical (SQM) procedure [12], using a set of scaling factors as in Table 1 [13]. A detailed discussion of a choice of the scaling factors will be given elsewhere [14]. After replacing the calculated frequencies by peak functions (here gaussian function of the width of  $7\text{ cm}^{-1}$ ), the calculated and experimental spectra could be compared. The polarised spectra were prepared by dividing the calculated transition dipole moments into components along and perpendicular to the axis of the lowest moment of inertia of the optimal conformation.

**TABLE 1** Scaling Factors for the Scaled Quantum Mechanical (SQM) Procedure

Symmetry of modes	Scaling factor
X-Y stretching	0.9254
X-H stretching (aliph.)	0.8890
X-H stretching (arom.)	0.9150
X-Y-Z bending	0.9923
X-Y-H bending	0.9473
H-X-H bending	0.9171
out-of-plane	0.9711
NH <sub>2</sub> wagging	0.8358
X-O-H, X-N-H bending	0.9047
torsions of conjugated systems	0.9389
torsions of single-bonded systems	0.8980
linear deformations	0.8905

## 5. RESULTS

### 5.1. Comparison of Isotropic Spectra

Figure 2 shows a comparison of both, the experimental and the calculated spectra in the isotropic phase. Figure 2(b) shows the most important part of the spectra in a range of frequencies 1800–1575 cm<sup>-1</sup>, with all the carbonyl bands and C–C stretching vibration of aromatic rings. Due to the presence of <sup>13</sup>C isotope, the band from carbonyl vibration inside the molecular core, which normally appears at about 1740 cm<sup>-1</sup>[15,16], is now shifted to a lower frequency of 1700 cm<sup>-1</sup>. Spectra of a member of the homologous series of MHPOCBC, studied using FT-IR spectroscopy by Sigarev *et al.* could be compared in reference [16]. The advantage of investigating the sample with <sup>13</sup>C isotope is quite obvious.

### 5.2. Comparison of Polarised Spectra

In order to obtain orientational information about the liquid crystal from a homogenously aligned cell it is necessary to record the polarised spectra. It allows us to measure the components of the absorbance along and perpendicular to the optical axis. We can reproduce the polarised spectra using values of transition dipole moments obtained from density functional theory calculations. We assume a simple model that the absorbance component along the optical axis corresponds to the transition dipole moment component along the axis of the lowest moment of inertia and the absorbance component perpendicular to the optical axis corresponds to the transversal components

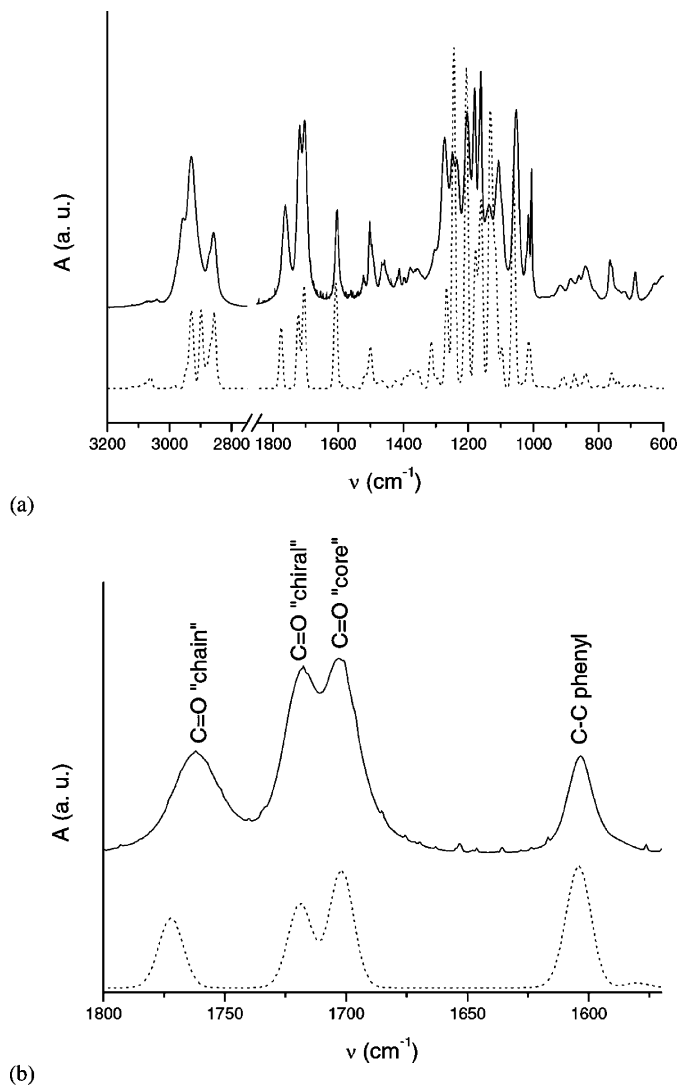


**FIGURE 2** Experimental and calculated spectra for the isotropic phase; (a) the whole Mid-IR region, (b) region of the C=O and C–C stretching vibrations, solid line – experimental spectrum, dotted line – calculated spectrum.

of the transition dipole moments. Then we assume a perfect orientational order and rotational freedom about the long molecular axis. Both assumptions are obviously false, but nevertheless we obtain very good agreement between experimental and calculated spectra, as

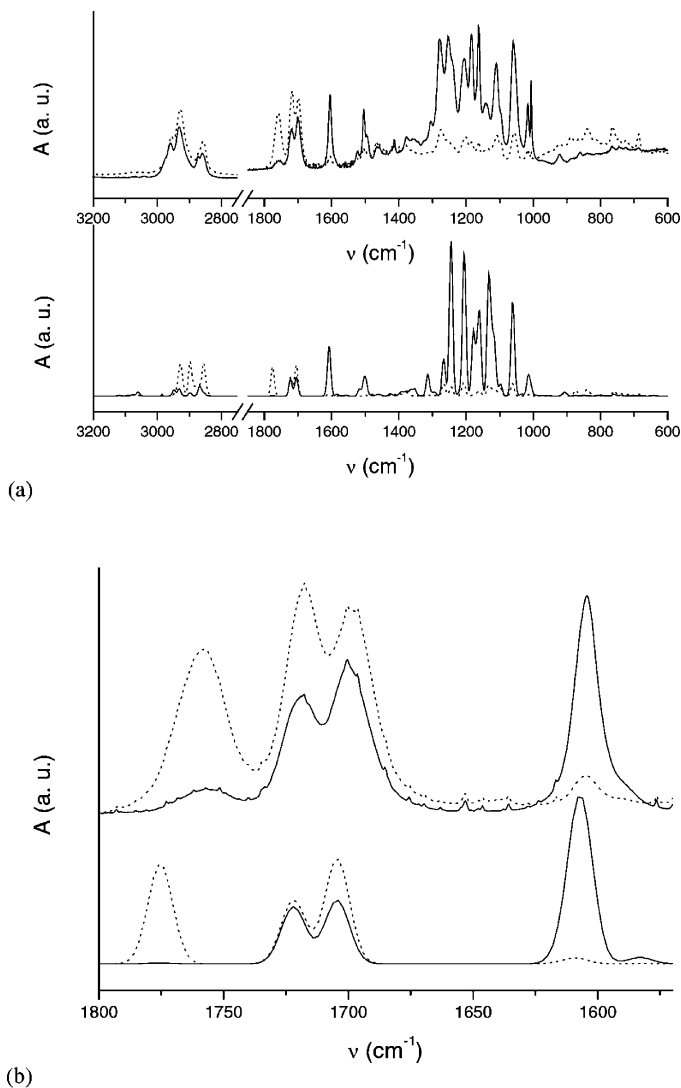


**FIGURE 3** Experimental and calculated polarised spectra for the smectic phase; (a) the whole Mid-IR region, (b) region of the C=O and C–C stretching vibrations, top plots – experimental spectra, bottom plots – calculated spectra, solid and dotted lines – longitudinal and transversal polarisation, respectively.

shown in Figure 3. The calculated spectra reproduce the experimental one and also values of the absorbance dichroic ratio (the ratio of longitudinal and perpendicular components of the absorbance) for con-



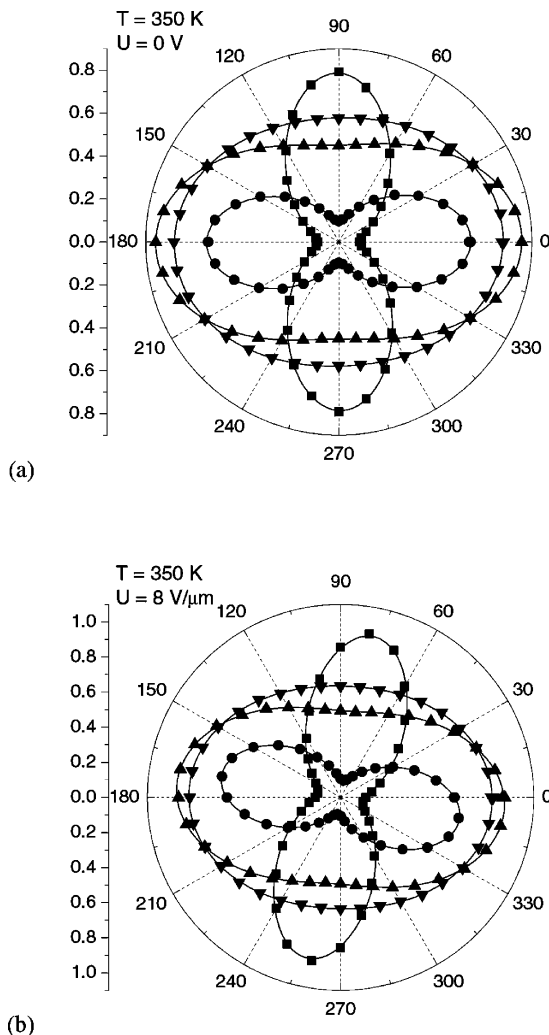


**FIGURE 4** Polar plots of the absorbance versus polarisation of the incident light without (a) and with (b) applied external electric field; squares – C–C stretching  $1600\text{ cm}^{-1}$ , circles, up triangles and down triangles – C=O stretching vibrations of the “chain” ( $1760\text{ cm}^{-1}$ ), “chiral” ( $1720\text{ cm}^{-1}$ ) and “core” ( $1700\text{ cm}^{-1}$ ) groups, respectively.

sidered stretching bands (Fig. 3 and 4). The dichroic ratio depends on the angle  $\beta$  between the transition dipole moment and the long molecular axis. The dipoles close to the “magic angle” [17–19] value of  $54.7^\circ$  (and  $\pi-54.7^\circ$ ), for which a uniaxial distribution about the long

**TABLE 2** Angles Between the Transition Dipole Moments and the Long Molecular Axis for Chosen Vibrational Bands

Vibration ( $\text{cm}^{-1}$ )	$\beta$ ( $^\circ$ )
1600	2.67
1700	52.2
1720	133.3
1760	95.4

axis is isotropic, exhibit dichroic ratio = 1. In our case the smallest value of the dichroic ratio corresponds to the band of the “core” carbonyl group. The calculated value of the angle  $\beta$  for this transition dipole moment is  $52.2^\circ$ . We may conclude that calculated values of angles  $\beta$  of transition dipole moments are reasonably close to the real values. The values for the bands under consideration are given in Table 2. It should be indicated that according to Osipov’s model of antiferroelectricity, the perpendicular orientation of the carbonyl group in the non-chiral chain favours anticlinic order and increases the “antiferroelectric strength”. We can analyse similar compounds:

- (i) MHPOBC with absence of such a dipole,
- (ii) MHP10CBC (reference [16]) with a longer non-chiral chain.

In both samples we can expect, that interactions between transversal dipoles, promoting antiferroelectricity, will be lower then in the case of the MHPOCBC and indeed both compounds exhibit rich polymorphism, including ferroelectric and several ferrielectric phases. Therefore we may conclude important role of these dipoles in forming antiferroelectricity. Moreover, only transversal components of such dipoles contribute to the interaction promoting antiferroelectricity. In our case, the perpendicularity of the dipole results in maximal efficiency of such an interaction. Similar situation, also seen by infrared spectroscopy and DFT calculations exist in a case of the Ajinomoto sample [18–20]. This material exhibits direct transition from the antiferroelectric  $\text{SmC}_A^*$  to the paraelectric  $\text{SmA}$  phase. We can conclude, that its “antiferroelectric strength” is even larger than that of the MHPOCBC.

### 5.3. Rotational Bias of Carbonyl Dipoles About the Long Molecular Axis

Application of an external electric field in the anticlinic antiferroelectric  $\text{SmC}_A^*$  phase above the threshold value induces transition to the

**TABLE 3** Angles of the Rotation of Absorbance Profiles for Chosen Vibrational Bands

Vibration ( $\text{cm}^{-1}$ )	$\theta$ ( $^{\circ}$ )
1600	12.2
1700	3.7
1720	5.0
1760	11.1

synclonic phase [9]. The absorbance profile rotates by an angle, which is close to the tilt angle of the molecule. In a case of the free rotation about the long molecular axis all the absorbance profiles should rotate about the same angle. The observed differences (Fig. 4, Table 3) indicate, that the rotation is biased [1,2,19,20].

## CONCLUSIONS

Infrared spectroscopic study of samples with selected carbon atoms exchanged by the  $^{13}\text{C}$  isotope is a very promising way in obtaining more detailed information about liquid crystalline systems. The infrared spectroscopy, when significantly supported by the density functional theory, is a powerful experimental technique for investigating the phase behaviour of antiferroelectric liquid crystals. During the last 15 years since the discovery of antiferroelectricity in liquid crystals, through several steps involving experiments and theory, we are now closer to understanding the origin of this phenomenon.

## REFERENCES

- [1] Kim, K. H., Ishikawa, K., Takezoe, H., & Fukuda, A. (1995). *Phys. Rev. E*, 51, 2166.
- [2] Kocot, A., Vij, J. K., & Perova, T. (2000). *Adv. Chem. Phys.*, 113, 203.
- [3] Osipov, M. A. & Fukuda, A. (2000). *Phys. Rev. E*, 62, 3724.
- [4] Osipov, M. A., Fukuda, A., & Hakoi, H. (2003). *Mol. Cryst. Liq. Cryst.*, 402, 9.
- [5] Isozaki, T., Suzuki, Y., Kawamura, I., Mori, K., Yamamoto, N., Yamada, Y., Orihara, H., & Ishibashi, Y. (1991). *Jap. J. Appl. Phys.*, 30, L1573.
- [6] Isozaki, T., Fujikawa, T., Takezoe, H., Fukuda, A., Hagiwara, T., Suzuki, Y., & Kawamura, I. (1993). *Phys. Rev. B*, 48, 13439.
- [7] Chandani, A. D. L., Górecka, E., Ouchi, Y., Takezoe, H., & Fukuda, A. (1989). *Jap. J. Appl. Phys.*, 28, L1265.
- [8] Fukuda, A., Hakoi, H., Sato, M., & Osipov, M. A. (2003). *Mol. Cryst. Liq. Cryst.*, 398, 169.
- [9] Fukuda, A., Takanishi, Y., Isozaki, T., Ishikawa, K., & Takezoe, H. (1994). *J. Mat. Chem.*, 4, 997.
- [10] Gaussian 98 (Revision A.11), Frisch M. J. *et al.*, Gaussian, Inc., Pittsburgh PA, 1998.

- [11] Becke, A. D. (1988). *Phys. Rev. A*, 38, 3098; Lee, C., Yang, W., & Parr, R. G. (1988). *Phys. Rev. B*, 41, 785.
- [12] Pulay, P., Fogarasi, G., Pongor, G., Boggs, J. E., & Vargha, A. (1983). *J. Am. Chem. Soc.*, 105, 7037; Rauhut, G. & Pulay, P. (1995). *J. Phys. Chem.*, 99, 3093.
- [13] Baker, J., Jarzecki, A. A., & Pulay, P. (1998). *J. Phys. Chem. A*, 102, 1412; Katsyuba, S. A., Grunenberg, J., & Schmutzler, R. (2001). *J. Mol. Struct.*, 559, 315.
- [14] Korlacki, R., Merkel, K., Kocot, A., Wrzalik, R., Vij, J. K., Ossowska-Chruściel, M. D., & Chruściel, J. in preparation.
- [15] Kim, K. H., Takanishi, Y., Ishikawa, K., Takezoe, H., & Fukuda, A. (1994). *Liquid Crystals*, 16, 185; Miyachi, K., Matsushima, J., Takanishi, Y., Ishikawa, K., Takezoe, H., & Fukuda, A. (1995). *Phys. Rev. E*, 52, R2153; Kocot, A., Wrzalik, R., Orgasinska, B., Perova, T., Vij, J. K. & Nguyen, H. T. (1999). *Phys. Rev. E*, 59, 551; Sigarev, A. A., Vij, J. K., Panarin, Yu. P., & Goodby, J. W. (2000). *Phys. Rev. E*, 62, 2269; Verma, A. L., Zhao, B., Bhattacharjee, A., & Ozaki, Y. (2001). *Phys. Rev. E*, 63, 51704.
- [16] Sigarev, A. A., Vij, J. K., Panarin, Yu. P., Rudquist, P., Lagerwall, S. T., & Heppke, G. (2003). *Liquid Crystals*, 30, 149.
- [17] Jang, W. G., Park, C. S., Kim, K. H., Glaser, M. A., & Clark, N. A. (2000). *Phys. Rev. E*, 62, 5027.
- [18] Jang, W. G. (2001). *J. Korean Phys. Soc.*, 38, 346.
- [19] Matsushima, J., Takanishi, Y., Ishikawa, K., Takezoe, H., Fukuda, A., Park, C. S., Jang, W. G., Kim, K. H., MacLennan, J. E., Glaser, M. A., Clark, N. A., & Takahashi, K. (2002). *Liquid Crystals*, 29, 27.
- [20] Jang, W. G., Park, C. S., MacLennan, J. E., Kim, K. H., & Clark, N. A. (1996). *Ferroelectrics*, 180, 213.